


Cite this: *RSC Adv.*, 2021, 11, 14568

# A facile preparation of immobilized naringinase on polyethyleneimine-modified Fe<sub>3</sub>O<sub>4</sub> magnetic nanomaterials with high activity

Chan Yu,<sup>a</sup> Qian Li,<sup>a</sup> <sup>a</sup> Jing Tian,<sup>a</sup> Honglei Zhan,<sup>a</sup> Xinyu Zheng,<sup>a</sup> Shujing Wang,<sup>a</sup> Xitong Sun<sup>\*b</sup> and Xiyang Sun<sup>\*c</sup>

Polyethyleneimine-modified Fe<sub>3</sub>O<sub>4</sub> nanoparticles (Fe<sub>3</sub>O<sub>4</sub>-PEI) were synthesized by the one-step co-precipitation method, and the resulting material was used to immobilize naringinase from the fermentation broth of *Aspergillus niger* FFCC uv-11. The immobilized naringinase activity could reach up to 690.74 U per g-support at the conditions of initial naringinase activity of 406.25 U mL<sup>-1</sup>, immobilization time of 4 h, glutaraldehyde concentration of 40% (w/v), immobilization temperature of 35 °C, and pH value of 5.5, with naringinase-carrying rate and naringinase activity recovery of 92.93% and 20.89%, respectively. In addition, the immobilized naringinase exhibited good pH and temperature stability in a pH range of 3.5–6.0 and temperature range of 40–70 °C, and the optimal reaction pH and reaction temperature were optimized as 5.5 and 60 °C, respectively. Besides, the immobilized naringinase could maintain 60.58% of the original activity after 10 reuse cycles, indicating that the immobilized naringinase had good reusability. Furthermore, the immobilized naringinase also performed excellent storage stability, 87.52% of enzyme activity still remained as stored at 4 °C for one month. In conclusion, the Fe<sub>3</sub>O<sub>4</sub>-PEI could be considered as a promising support for naringinase immobilization, with the advantages of high enzyme activity loading, good reusability, storage stability and rapid recovery.

Received 23rd February 2021  
Accepted 13th April 2021

DOI: 10.1039/d1ra01449h

rsc.li/rsc-advances

## 1. Introduction

The bitterness of citrus fruits (mainly grapefruit) is one of the major limiting factors in the development of the juice industry.<sup>1</sup> The hydrolysis of bitter components by naringinase was considered as a promising method for the juice debittering, since it not only enhanced the sensory properties, but also preserved the properties of health promotion,<sup>2</sup> which had attracted more and more interest of biological researchers. Naringinase is composed of  $\alpha$ -L-rhamnosidase (EC 3.2.1.40) and  $\beta$ -D-glucosidase (EC 3.2.1.21) to form a hydrolytic multi-enzyme complex,<sup>3</sup> and the  $\alpha$ -L-rhamnosidase catalyzes the hydrolysis of naringin (naringenin 7-rhamnoglucoside) into rhamnose and prunin (4,5,7-trihydroxy flavanone-7-glucoside); the prunin is then altered to naringenin (4,5,7-trihydroxy flavanone) and glucose by the  $\beta$ -D-glucosidase activity at the same time.<sup>4,5</sup> Because hydrolyzed products from naringin could effectively

promote health, naringinase is widely used in the pharmaceutical, cosmetic and food industries.<sup>6</sup> However, there were many practical problems in the use of free enzymes, including not repeating use of enzymes, environmental sensitivity and difficulty in enzyme separation. Compared with free enzymes, the immobilized enzymes had the advantages of easy separation, low total reaction cost, and could enhance the stability and reusability of the enzymes, especially in the large-scale applications. In recent years, several methods for immobilizing enzymes have been developed, such as covalent, multivalent, ionic binding, adsorption or cross-linking and encapsulation (encapsulation) methods.<sup>7</sup> In the food industry, cheap immobilization conditions and easily available immobilized enzymes were the important choice for the use of immobilized enzymes, which meant that the support must contain readily available reactive groups to achieve simple and inexpensive activation, and must be completely non-toxic and have sufficient stability.<sup>1</sup>

Up to now, naringinase had been successfully immobilized on different types of carriers, such as porous glass beads, chitin, diatomaceous earth, glutaraldehyde-coated wood chips, alginic acid salt,<sup>8–10</sup> mesoporous silica materials, polyvinyl alcohol and other polymeric materials.<sup>11</sup> Recently, in the progress of immobilization technology and materials,<sup>12</sup> the rapid and extensive development of nano-sized particles (NPs) attracted a lot of attention.<sup>13</sup> Among them, iron oxide nanoparticles were of great interest in the food industry due to the outstanding

<sup>a</sup>School of Biological Engineering, Dalian Polytechnic University, No. 1st Qinggongyuan, Ganjingzi, Dalian 116034, P. R. China. E-mail: liqian19820903@163.com; Fax: +86-411-86323725; Tel: +86-411-86323725

<sup>b</sup>School of Light Industry & Chemical Engineering, Dalian Polytechnic University, No. 1st Qinggongyuan, Ganjingzi, Dalian 116034, P. R. China. E-mail: xitongsun@163.com; xiyang@ucr.edu

<sup>c</sup>Department of Chemical and Environmental Engineering, University of California Riverside, Riverside, CA 92521, USA



features including super paramagnetism and low toxicity. The magnetic nanoparticles (MNP) could be coated with biocompatible and diamagnetic materials (such as organic polymers or silica shells) to inhibit the formation of large aggregates of MNP, which could be further used to promote the function of adhesion.<sup>14</sup> The high specific surface area of MNP improved the binding efficiency of enzymes, and the super paramagnetic behavior supported the rapid and selective recovery using magnet.<sup>15–19</sup> Naringinase and lysine-assisted magnetic nanoparticles were covalently combined to produce nano magnetic cross-linked enzyme aggregates (NM-NGase-CLEAs).<sup>18</sup> Cross-linking agents used for surface modification of magnetic nanoparticles, such as silanization or carbodiimide activation, contributed to enzyme binding and stabilization.<sup>20</sup> Polyethyleneimine (PEI), as polycationic polymer, had many advantages, including good water solubility, high functional group content, fit molecular weight, and good physical and chemical stability.<sup>21,22</sup> PEI could be used to modify enzymes through its amine groups,<sup>23</sup> and could also be transplanted to the support and then cross-linked by bifunctional agent, which would be widely used to immobilize various enzymes.<sup>24</sup>

In this study, we focused on the immobilized enzyme formed by covalent linking between  $\text{Fe}_3\text{O}_4$  nanoparticles modified by PEI (marked as  $\text{Fe}_3\text{O}_4\text{-PEI}$ ) and naringinase. The material was first prepared by one-step co-precipitation method, and subsequently characterized including transmission electron microscopy, infrared spectroscopy, elemental analysis, magnetic property and zeta potential. In order to further understand the characteristics and hydrolysis performance of naringinase immobilized on this material, the optimization experiments including initial enzyme activity, immobilization temperature, immobilization pH, glutaraldehyde concentration and immobilization time was investigated. In addition, the temperature and pH stability, reusability and storage stability of the immobilized enzyme were also studied.

## 2. Materials and methods

### 2.1 Materials

*Aspergillus niger* FFCC uv-11 was stored in our laboratory, and the naringinase fermentation broth was produced *via* the strain with a naringinase activity of 650.0 U mL<sup>-1</sup>. Naringin (mass fraction  $\geq 98\%$ ) was purchased from Baoji Fang Sheng Biological development Co., Ltd, China. Polyethyleneimine (M.W. 10 000 Da, 99%) was obtained from Aladdin Inc. Sodium hydroxide, anhydrous ethanol, citric acid, disodium hydrogen phosphate, diethylene glycol, glutaraldehyde (50% by mass),

trisodium citrate and ammonia ( $\text{NH}_3\cdot\text{H}_2\text{O}$ , 25%, w/v) were purchased from Tianjin Damao Chemical Reagent Co., Ltd. Anhydrous ferric chloride ( $\text{FeCl}_3$ ) and ferrous sulfate heptahydrate ( $\text{FeSO}_4\cdot 7\text{H}_2\text{O}$ ) were supplied by Sinopharm Chemical Reagent Co., Ltd.

### 2.2 Preparation of $\text{Fe}_3\text{O}_4\text{-PEI}$ material

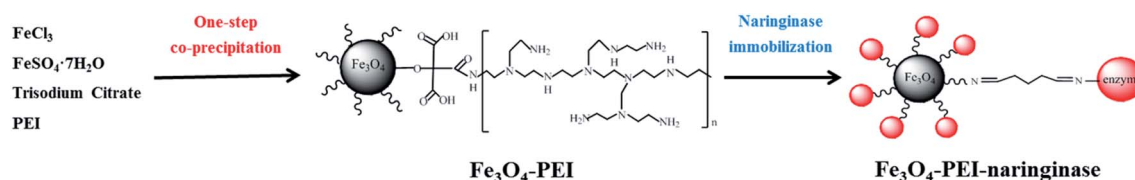
The PEI modified  $\text{Fe}_3\text{O}_4$  material ( $\text{Fe}_3\text{O}_4\text{-PEI}$ ) was prepared by the one-step co-precipitation method (Scheme 1). First, an amount of 400 mL of deionized water was added into a 1000 mL round bottom flask, and 5.63 g of anhydrous ferric chloride and 5.0 g of ferrous sulfate heptahydrate were then added into the flask. The mixture was heated up to 85 °C for 30 min under nitrogen atmosphere. Subsequently, 100 mL of  $\text{NH}_3\cdot\text{H}_2\text{O}$  was added into the above mixture under vigorous stirring. After one minute, 0.306 g of trisodium citrate was quickly added into the mixture. Finally, 10.4 g of PEI (molecular weight of 10 000) was added into the mixture, and kept reacting for 2 hours.<sup>25</sup> The resulting PEI-modified  $\text{Fe}_3\text{O}_4$  magnetic nanoparticles (marked as  $\text{Fe}_3\text{O}_4\text{-PEI}$ ) were separated by an magnet and washed three times with ethanol and deionized water, and then stored in deionized water at 4 °C.

### 2.3 Preparation of immobilized naringinase

An amount of 0.2 g of  $\text{Fe}_3\text{O}_4\text{-PEI}$  material was mixed with 2 mL of naringinase fermentation broth, and then 6 mL of citrate buffer was added to adjust the pH to 4.5. Then 1 mL of glutaraldehyde was added for cross-linking. In addition, the mixture was shaken at a constant temperature of 160 rpm for 4 hours, and was separated by magnet precipitation. Furthermore, the separated material was washed with deionized water for three times. After that, the material was marked as  $\text{Fe}_3\text{O}_4\text{-PEI-naringinase}$  and stored in deionized water at 4 °C for later use.

### 2.4 Determination of immobilized naringinase activity

The modified Davis method was used for the determination of naringinase activity:<sup>26</sup> 0.8 mL of naringin solution (naringin concentration of 0.8 g L<sup>-1</sup>, pH of 4.5) was added to 30 mg of immobilized naringinase or 0.2 mL of free naringinase, and then the mixture was placed in a water bath at 50 °C for 30 minutes. Finally, 0.1 mL of the above mixture and 0.1 mL of NaOH solution (with the concentration of 4 mol L<sup>-1</sup>) were added into 5 mL of diethylene glycol (90%, v/v), and the absorbance of the solution was measured at 420 nm.



**Scheme 1** Schematic diagram of the preparation process and mechanism for the immobilized naringinase on PEI-modified  $\text{Fe}_3\text{O}_4$  magnetic nanoparticles ( $\text{Fe}_3\text{O}_4\text{-PEI-naringinase}$ ).

**Definition of naringinase activity (U).** The amount of naringinase required to degrade 1 mg of naringin per minute at pH 4.5 and 50 °C was defined as one unit of naringinase activity. The definition of specific enzyme activity (U per g-support or U mL<sup>-1</sup>): the enzyme activity that degrades 1 g of immobilized naringinase (or 1 mL of free naringinase) per minute at pH 4.5 and 50 °C. The experiments were carried out in triplicate.<sup>11,27,28</sup>

## 2.5 Study on the enzymatic properties of immobilized naringinase

The effect of reaction temperature on immobilized naringinase: 30 mg of immobilized naringinase (or 0.2 mL of free naringinase) was added to 0.8 mL of naringin solution with the pH value of 4.5. The mixture was subjected to the hydrolysis temperature of 40, 45, 50, 55, 60, 65 and 70 °C, respectively, and the relative enzyme activity was measured.

The effect of pH on immobilized naringinase: 30 mg immobilized naringinase (or 0.2 mL free naringinase) was added to 0.8 mL naringin solution (the pH value of the solution was adjusted to 3.0, 3.5, 4.0, 4.5, 5.0, 5.5, 6.0 by citric acid buffer, respectively). The mixture was kept at 50 °C for the hydrolysis reaction, and then the relative enzyme activity was measured.

Storage stability of immobilized naringinase: immobilized naringinase and free naringinase were stored at 4 °C for 30 days, and the activities of them were measured every 5 days.

Repeated use of immobilized naringinase: the operational stability of the immobilized enzyme was determined to quantify the reduction in naringin. At 55 °C, 30 mg of immobilized naringinase was mixed with 0.8 mL of naringin solution (pH of 5.5) for 30 minutes, and it was continuously reused. After each cycle, the immobilized naringinase are separated with a strong magnet, and then proceed to the next cycle.

## 2.6 Calculation of naringinase-carrying rate and naringinase activity recovery

Naringinase-carrying rate (*B*) was determined by the following equation:<sup>29</sup>

$$B/\% = (A_0 - A_1)/A_0 \times 100 \quad (1)$$

wherein, *B* represents the carrying rate of naringinase, *A*<sub>0</sub> refers to the total enzyme activity in the enzyme solution before fixation, and *A*<sub>1</sub> refers to the total enzyme activity remaining in the supernatant after fixation.

Immobilized naringinase activity recovery (*R*) was obtained by the following equation:

$$R/\% = A_2/(A_0 - A_1) \times 100 \quad (2)$$

where *R* represents the recovery rate of naringinase, *A*<sub>0</sub> and *A*<sub>1</sub> are the same as eqn (1). *A*<sub>2</sub> refers to the total activity of the immobilized naringinase in the enzymatic reaction, that is, the total enzyme activity measured in the enzymatic hydrolysis reaction.

Relative naringinase activity (*Q*) was calculated by the following equation:

$$Q/\% = P/K \times 100 \quad (3)$$

wherein, *Q* represents the relative enzyme activity, *P* refers to the enzyme activity under certain conditions, and *K* refers to the highest enzyme activity under the same conditions.

## 2.7 Characterization of materials

The morphology of Fe<sub>3</sub>O<sub>4</sub>-PEI magnetic particles were characterized by transmission electron microscopy (TEM, JEOL JEM-2100F). A Spectrum 10 spectrophotometer (PerkinElmer, USA) was used to record the Fourier transform infrared (FT-IR) spectra of Fe<sub>3</sub>O<sub>4</sub>, Fe<sub>3</sub>O<sub>4</sub>-PEI and Fe<sub>3</sub>O<sub>4</sub>-PEI-naringinase between 400 and 4000 cm<sup>-1</sup> with a resolution of 2 cm<sup>-1</sup>. The elemental composition (N, C and H) of Fe<sub>3</sub>O<sub>4</sub>-PEI and Fe<sub>3</sub>O<sub>4</sub>-PEI-naringinase material were tested by using an elemental analyzer (Elementar: Vario EL cube). A vibrating sample

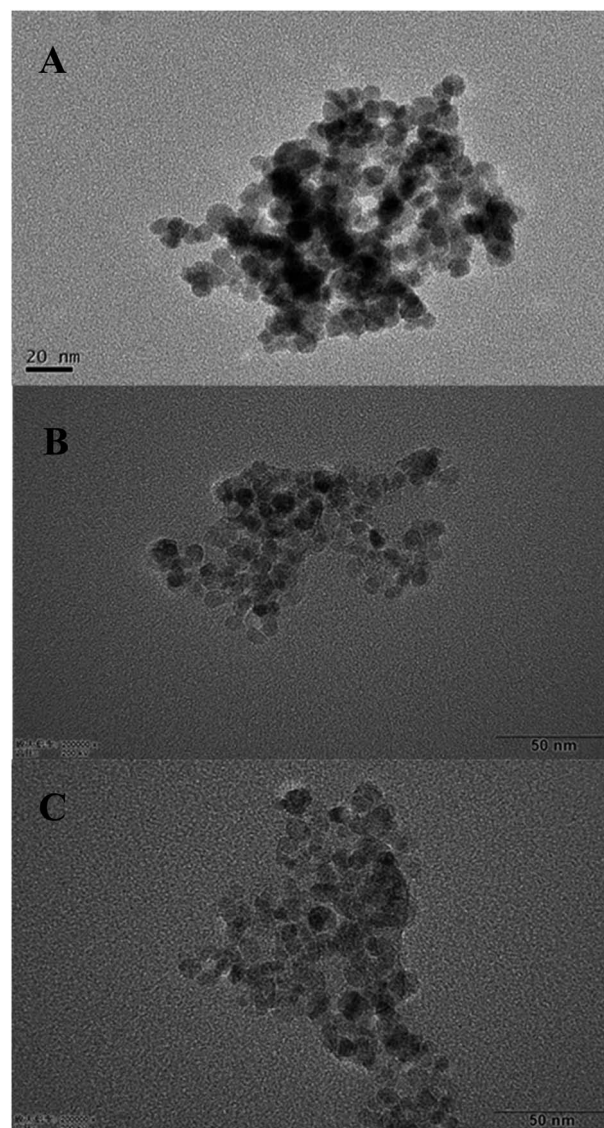


Fig. 1 TEM images of Fe<sub>3</sub>O<sub>4</sub> (A), Fe<sub>3</sub>O<sub>4</sub>-PEI (B) and Fe<sub>3</sub>O<sub>4</sub>-PEI-naringinase (C).





magnetometer (LakeShore-7400S) was used to measure the magnetic hysteresis loop of  $\text{Fe}_3\text{O}_4$ -PEI. The zeta potential of  $\text{Fe}_3\text{O}_4$ -PEI was analyzed by using a laser particle size analyzer (Zetasizer 3000HSA). The nitrogen adsorption/desorption isotherms were measured on a QuantaChrome Quadrasorb SI analyzer (USA) after vacuum degassing at 120 °C for 6 h, and the specific surface areas were calculated using the Brunauer–Emmett–Teller (BET) method. X-ray diffractometer (D/max3B) was used to characterize the crystal structure of  $\text{Fe}_3\text{O}_4$ -PEI. The thermogravimetric analysis of  $\text{Fe}_3\text{O}_4$ -PEI-naringinase (TGA, Netzsch STA 449C, Germany) was carried out under the conditions of air atmosphere from room temperature to 1000 °C with a heating rate of 10 °C min<sup>-1</sup>.

### 3. Results and discussion

#### 3.1 Characterization of materials

The TEM images of  $\text{Fe}_3\text{O}_4$  (A),  $\text{Fe}_3\text{O}_4$ -PEI (B) and  $\text{Fe}_3\text{O}_4$ -PEI-naringinase (C) were shown in Fig. 1. The average diameter of  $\text{Fe}_3\text{O}_4$  and  $\text{Fe}_3\text{O}_4$ -PEI nanoparticles were estimated about 10 nm, which was smaller than the theoretical diameter of the single domain superparamagnetic  $\text{Fe}_3\text{O}_4$  particles (25 nm), indicating that the  $\text{Fe}_3\text{O}_4$ -PEI nanoparticles had superparamagnetic characteristics. It could be seen from Fig. 1C that the surface morphology of  $\text{Fe}_3\text{O}_4$ -PEI-naringinase was similar with those of  $\text{Fe}_3\text{O}_4$  and  $\text{Fe}_3\text{O}_4$ -PEI. In addition, it suggested in Fig. 2 that the magnetic hysteresis loop of  $\text{Fe}_3\text{O}_4$ -PEI had no hysteresis. The enlarged view of M–H of  $\text{Fe}_3\text{O}_4$ -PEI was shown in Fig. 2C. When the external magnetic field  $H = 0$ , the remanence magnetization ( $M_r$ ) and the variations of coercivity ( $H_c$ ) were both nearly zero, proving that the  $\text{Fe}_3\text{O}_4$ -PEI nanoparticles had good superparamagnetism. The saturation magnetization ( $M_s$ ) was evaluated as 65.385 emu g<sup>-1</sup>. With such high  $M_s$ , the microspheres showed a high magnetic responsiveness and could be quickly separated from the aqueous solution by a magnet.

It could be seen that the strong band at 582 cm<sup>-1</sup> vibration was corresponded to the Fe–O bond,<sup>30</sup> and the bands at

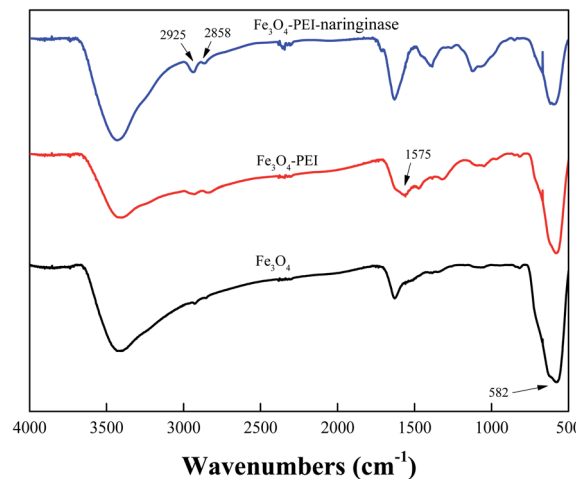


Fig. 3 FT-IR spectra of  $\text{Fe}_3\text{O}_4$ ,  $\text{Fe}_3\text{O}_4$ -PEI and  $\text{Fe}_3\text{O}_4$ -PEI-naringinase.

2925 cm<sup>-1</sup> and 2858 cm<sup>-1</sup> were characteristics of C–H bond.<sup>30,31</sup> In contrast, in the FT-IR spectrum of  $\text{Fe}_3\text{O}_4$ -PEI-naringinase, the absorbance peaks of C–H band increased to a large degree, indicating that naringinase had been successfully immobilized on the  $\text{Fe}_3\text{O}_4$ -PEI. In addition, the new band appeared at 1575 cm<sup>-1</sup> might be corresponding to the N–H vibration in the FT-IR spectrum of  $\text{Fe}_3\text{O}_4$ -PEI.<sup>32</sup> It was shown that  $\text{Fe}_3\text{O}_4$  particles were successfully modified with PEI through covalent bands (Fig. 3).

The results of zeta potential of  $\text{Fe}_3\text{O}_4$ -PEI nanoparticles at the pH range of 8–12 was shown in Fig. 4. It was obvious that the zeta potential increased with the decrease of pH value. The isoelectric point (pI) was found at 10, which was attributed to the protonation of a large number of amino groups on the PEI molecule. This result also revealed that the PEI was successfully modified on the  $\text{Fe}_3\text{O}_4$  nanoparticles.

The result of elemental analysis was shown in Table 1. It was clear that the  $\text{Fe}_3\text{O}_4$ -PEI had a high amino group content, with the N content of 3.945%. Compared with the  $\text{Fe}_3\text{O}_4$ -PEI, the contents of N, C and H in  $\text{Fe}_3\text{O}_4$ -PEI-naringinase remarkably

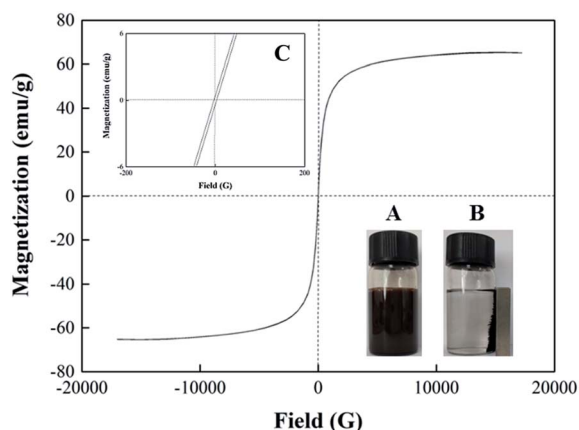


Fig. 2 Magnetic hysteresis loop of  $\text{Fe}_3\text{O}_4$ -PEI; the inset (C) demonstrates the magnetic separation of  $\text{Fe}_3\text{O}_4$ -PEI magnetic particles from aqueous solution under an external magnetic field and the time from (A) to (B) was less than 20 s.

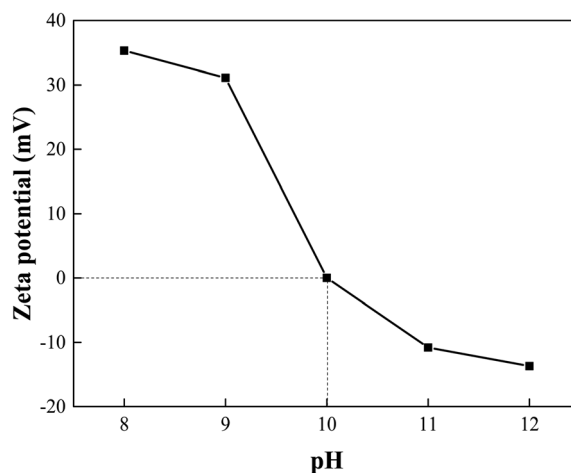


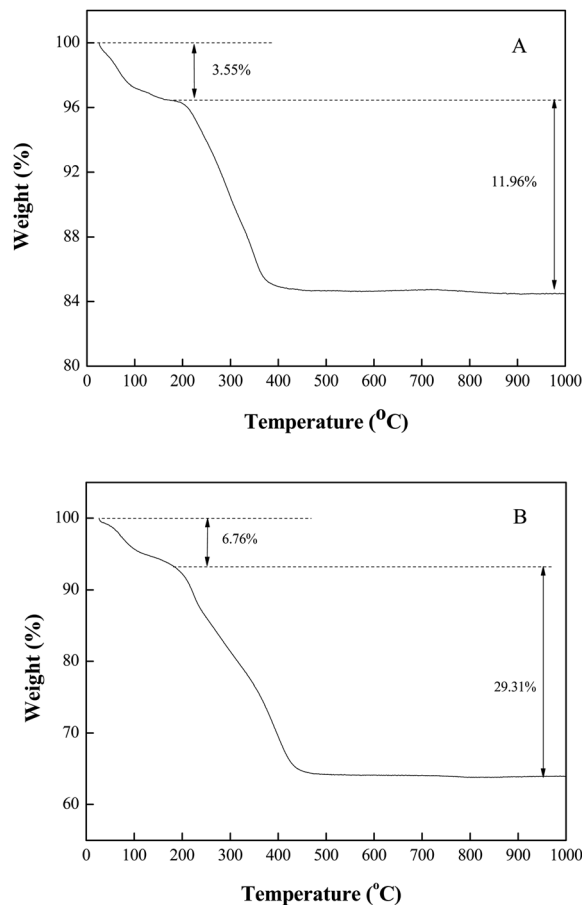
Fig. 4 Zeta potential of  $\text{Fe}_3\text{O}_4$ -PEI at variable pH values.

**Table 1** Elemental analysis and specific surface area of Fe<sub>3</sub>O<sub>4</sub>, Fe<sub>3</sub>O<sub>4</sub>-PEI and Fe<sub>3</sub>O<sub>4</sub>-PEI-naringinase

Samples	N (%)	C (%)	H (%)	Specific surface area (m <sup>2</sup> g <sup>-1</sup> )
Fe <sub>3</sub> O <sub>4</sub>	N.A.	N.A.	N.A.	137.7
Fe <sub>3</sub> O <sub>4</sub> -PEI	3.945	6.690	1.847	108.1
Fe <sub>3</sub> O <sub>4</sub> -PEI-naringinase	4.582	18.957	2.789	91.0

increased up to 4.582%, 18.957%, 2.789%, respectively, implying that naringinase was successfully immobilized on Fe<sub>3</sub>O<sub>4</sub>-PEI material. In addition, the specific surface area of Fe<sub>3</sub>O<sub>4</sub>, Fe<sub>3</sub>O<sub>4</sub>-PEI and Fe<sub>3</sub>O<sub>4</sub>-PEI-naringinase was characterized by the nitrogen adsorption/desorption isotherms. It was clear that the Fe<sub>3</sub>O<sub>4</sub>-PEI had a high specific surface area, and was suitable for the enzyme immobilization. Besides, the specific surface area decreased from 137.7 (Fe<sub>3</sub>O<sub>4</sub>) to 108.1 m<sup>2</sup> g<sup>-1</sup> (Fe<sub>3</sub>O<sub>4</sub>-PEI), suggesting that the PEI was effectively modified on the surface of Fe<sub>3</sub>O<sub>4</sub>, and the lowest specific surface area of Fe<sub>3</sub>O<sub>4</sub>-PEI-naringinase indicated that the naringinase was successfully immobilized on the material.

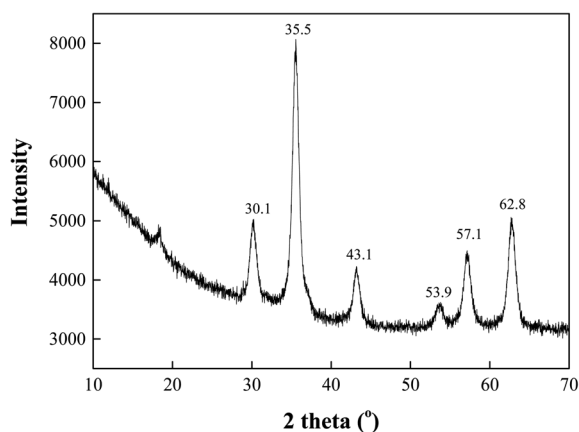
The X-ray diffraction pattern of Fe<sub>3</sub>O<sub>4</sub>-PEI was shown in Fig. 5, which was used to characterize its crystal structure. The six characteristic peaks appeared in Fe<sub>3</sub>O<sub>4</sub>-PEI at 30.1°, 35.5°, 43.1°, 53.9°, 57.1° and 62.8° were assigned to (220), (311), (400), (422), (511) and (440) planes of the pure Fe<sub>3</sub>O<sub>4</sub> (JCPDS card no. 65-3107).<sup>33</sup> In addition, the thermogravimetric analysis of Fe<sub>3</sub>O<sub>4</sub>-PEI and Fe<sub>3</sub>O<sub>4</sub>-PEI-naringinase were also investigated. As shown in Fig. 6A, it could be seen that the weight loss occurred in two different stages in the TGA curve of Fe<sub>3</sub>O<sub>4</sub>-PEI, and the residual weight was 84.49%. In the first stage, from 30 °C to 180 °C, the weight loss was about 3.55%, which was equivalent to the loss of adsorbed and bound water on the nanoparticles. The second stage of weight loss of 11.96% started at about 180 °C and ended at 840 °C, which was attributed to the thermal decomposition of the surface citric acid and polyethyleneimine. Fig. 6B showed the TGA curve of Fe<sub>3</sub>O<sub>4</sub>-PEI-naringinase, the weight loss occurred also in two

**Fig. 6** The TGA curves of Fe<sub>3</sub>O<sub>4</sub>-PEI (A) and Fe<sub>3</sub>O<sub>4</sub>-PEI-naringinase (B).

different stages, and the residual weight was 63.93%, which was much lower than that of Fe<sub>3</sub>O<sub>4</sub>-PEI. From the above data, it could be preliminarily calculated that the content of naringinase on Fe<sub>3</sub>O<sub>4</sub>-PEI nanoparticles was 24.33%, with the naringinase loading amount of 0.32 g per g-support. This results also proved that the synthetic method was feasible and the immobilization was successful.

### 3.2 Optimization of immobilization parameters

**3.2.1 Effect of the initial naringinase activity.** As shown in Fig. 7A, the immobilized naringinase activity increased with the initial naringinase activity increased from 162.50 U mL<sup>-1</sup> to 406.25 U mL<sup>-1</sup>. When the initial naringinase activity was 406.25 U mL<sup>-1</sup>, the immobilized naringinase activity reached the maximum of 624.86 U per g-support. Additionally, the activity of immobilized naringinase decreased as the initial naringinase activity increased from 406.25 U mL<sup>-1</sup> to 650.00 U mL<sup>-1</sup>. It might because a large number of naringinase was bound to the carrier, which increased the steric hindrance and diffusion restriction among enzyme molecular, and further induced the difficulty of contact between enzyme and substrate. As a result, the immobilized naringinase activity increased slowly or even decreased.<sup>34</sup>

**Fig. 5** XRD patterns of Fe<sub>3</sub>O<sub>4</sub>-PEI.

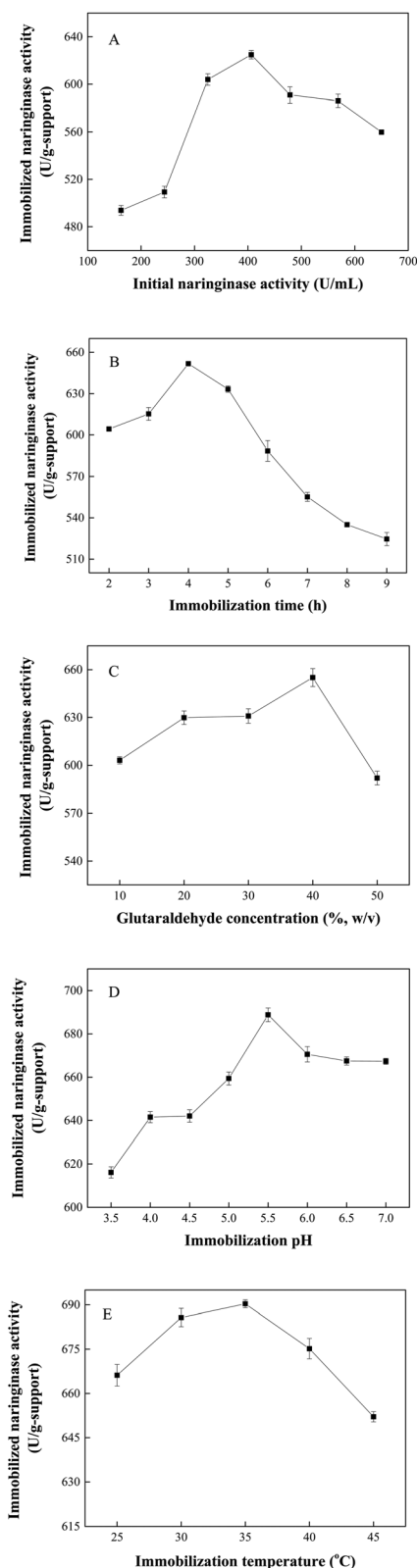


Fig. 7 The effect of initial naringinase activity (A), immobilization time (B), glutaraldehyde concentration (C), immobilization pH (D) and immobilization temperature (E) on  $\text{Fe}_3\text{O}_4$ -PEI-naringinase activity.

**3.2.2 Effect of immobilization time.** The effect of immobilization time on immobilized naringinase activity was shown in Fig. 7B and the optimized immobilization time was 4 h. It could be seen that in the immobilization time range of 2–4 h, the immobilized naringinase activity was increased. It was illuminated that free naringinase required sufficient time to bind to the material. However, when the immobilization time exceeded 4 h, the immobilized naringinase activity decreased rapidly. It might be because when the immobilization time reached 4 h, the amount of immobilized naringinase on the carrier was saturated, and longer immobilization time would cause more naringinase to attach to the surface of the material. It might increase the steric hindrance between the naringinase molecules and cover part of the active center of naringinase, which made the immobilized naringinase activity reduced.<sup>35</sup>

**3.2.3 Effect of glutaraldehyde concentration.** The effect of glutaraldehyde concentration on immobilized naringinase activity was shown in Fig. 7C. As the concentration of glutaraldehyde gradually increased from 10% to 40% (w/v), the naringinase activity gradually increased and reached the maximum of 655.08 U per g-support at the glutaraldehyde concentration of 40%. Glutaraldehyde concentrations below 40% could not provide sufficient binding sites for naringinase, and resulted in lower naringinase activity. When the glutaraldehyde concentration was further increased from 40% to 50%, the naringinase activity was not further increased. On one hand, it might be due to the deactivation of the enzyme by excessive glutaraldehyde. On the other hand, high glutaraldehyde concentration might cause uncontrolled reaction, which induced polymerization of glutaraldehyde in the solution and decreased the immobilization efficiency.<sup>36</sup>

**3.2.4 Effect of immobilization pH.** It could be seen from Fig. 7D that the immobilized naringinase showed the highest naringinase activity at the pH value of 5.5. The ionization of certain groups in proteins could be affected by pH value. Under acidic condition, the positively charged naringinase would form a stable and insoluble co-aggregate with the positively charged PEI through covalent linkage. When the pH was too high or too low, aggregates could not be well formed due to the repulsion between the same charges, resulting in a decrease in the activity of the immobilized enzyme.<sup>37</sup>

**3.2.5 Effect of immobilization temperature.** The effect of immobilization temperature on immobilized naringinase activity was shown in Fig. 7E. It could be seen the immobilized naringinase activity increased as the temperature increased from 25 °C to 35 °C, and the optimized immobilization temperature was 35 °C. In the temperature range from 35 °C to 45 °C, the immobilized naringinase activity decreased slightly, which might be due to the temperature sensitivity of naringinase. Soria *et al.*<sup>8</sup> obtained a similar course of sensitivity characteristics of immobilized  $\alpha$ -L-rhamnosidase on ferromagnetic supports.

As mentioned above, the optimal parameters for naringinase immobilization were as follows: initial naringinase activity of  $406.25 \text{ U mL}^{-1}$ , immobilization time of 4 h, glutaraldehyde concentration of 40% (w/v), immobilization temperature of

35 °C, immobilization pH of 5.5. The naringinase-carrying rate, naringinase activity recovery and maximum  $\text{Fe}_3\text{O}_4$ -PEI-naringinase activity were 92.93%, 20.89% and 690.74 U per g-support, respectively. The immobilized naringinase activity in this work was higher than most of those in previous reports.<sup>7,8,38,39</sup>

### 3.3 Hydrolysis properties of $\text{Fe}_3\text{O}_4$ -PEI-naringinase

**3.3.1 The optimum enzymatic reaction conditions of  $\text{Fe}_3\text{O}_4$ -PEI-naringinase.** Fig. 8A showed that the optimal enzymatic reaction temperature of immobilized naringinase was 60 °C, while the optimal enzymatic reaction temperature of free naringinase was 50 °C under the same conditions. Compared with the free enzyme, the immobilized naringinase exhibited good thermal stability in the temperature range of 40–70 °C, which might be due to the covalent cross-linking between  $\text{Fe}_3\text{O}_4$ -PEI and primary amine, and glutaraldehyde promoted the tertiary structure of the enzyme through the amino group of the enzyme.<sup>38</sup> The results were similar to previous studies by Luo *et al.*<sup>40</sup> and Jordan,<sup>41</sup> because the immobilization of naringinase led to an increase in the optimal temperature compared to the free form.<sup>28</sup>

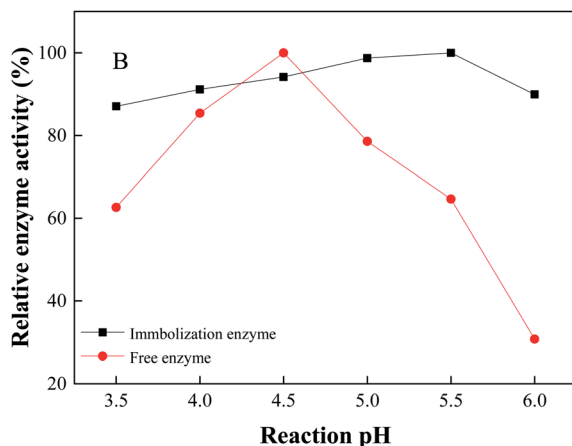
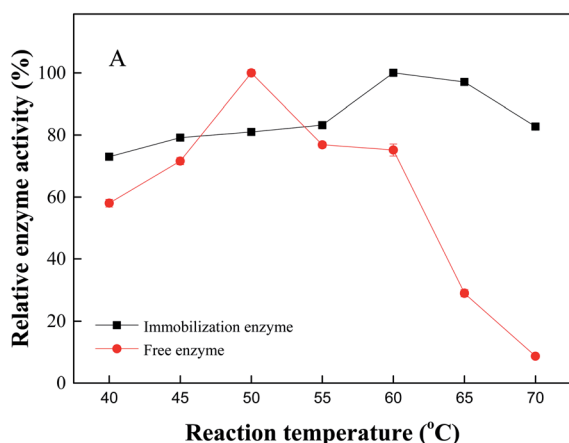


Fig. 8 The optimal enzymatic reaction temperature (A) and reaction pH (B) of the  $\text{Fe}_3\text{O}_4$ -PEI-naringinase and free naringinase.

Table 2 Comparison of enzyme activity of naringinase immobilized on different materials

Immobilized carrier	Naringinase activity	References
Poly(vinyl alcohol) cryogels	$1.10 \pm 0.02 \text{ U g}^{-1}$	28
Chitosan microspheres	$48.33 \text{ U g}^{-1}$	8
Silanized SBA-15	$517.43 \text{ U g}^{-1}$	39
PEI- $\text{Fe}_3\text{O}_4$	$710.97 \pm 6.13 \text{ U g}^{-1}$	This work

In Fig. 8B, the optimal enzymatic pH of immobilized naringinase was determined at a pH of 5.5, and the optimal enzymatic pH of free naringinase was 4.5. At the same time, it was found that the activity of immobilized naringinase was relatively stable under the same conditions, but the free enzyme fluctuated greatly. Therefore, it was indicated that  $\text{Fe}_3\text{O}_4$ -PEI-naringinase had a wide application pH range and good acid resistance.<sup>40</sup> Compared with free enzymes, the covalent bonding approach of immobilized enzymes provided a more stable pH-specific biocatalyst, which might be attributed to the restriction of conformational changes in pH changes.<sup>21</sup>

The enzyme activities of  $\text{Fe}_3\text{O}_4$ -PEI and other carriers for immobilized naringinase were summarized in Table 2, and the values of enzyme activity were given under the same unit. Compared with the previous literature (Table 2), the immobilized naringinase activity in this work was higher, which indicated that  $\text{Fe}_3\text{O}_4$ -PEI had good performance in naringinase immobilization.

**3.3.2 Reusability of the  $\text{Fe}_3\text{O}_4$ -PEI-naringinase.** The immobilized naringinase was prepared under the optimized immobilization conditions, and then was used for reusability test. It was shown in Fig. 9 that after ten cycles, 60.58% of the original enzyme activity was still retained. That might because large amount of multi-point covalent bonds were formed between the surface of the  $\text{Fe}_3\text{O}_4$ -PEI nanoparticles and naringinase, and led to the improvement of the stability of naringinase. Naringinase immobilized on  $\text{Fe}_3\text{O}_4$ -PEI would have great potential for development and application of naringinase.<sup>42</sup>

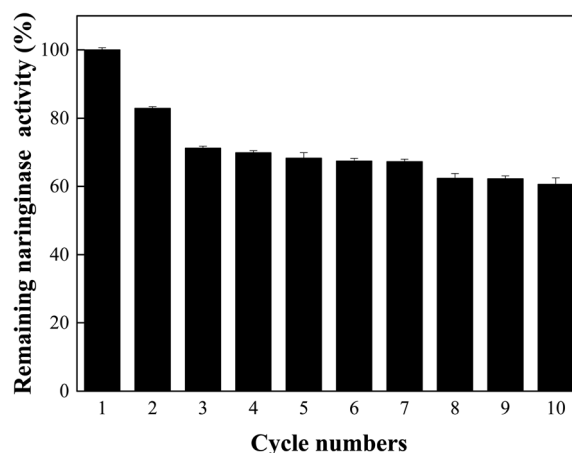


Fig. 9 The recycling of  $\text{Fe}_3\text{O}_4$ -PEI-naringinase.



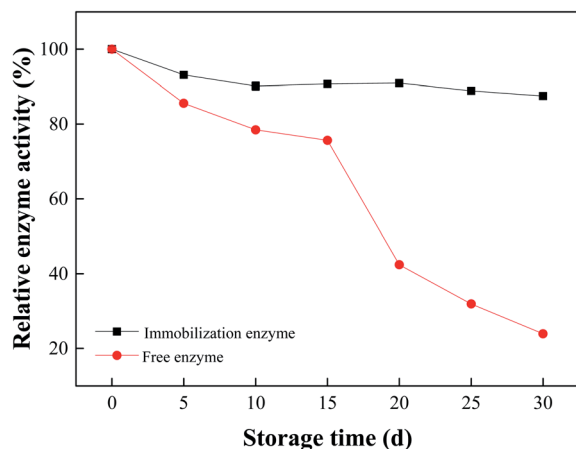


Fig. 10 Storage stability of  $\text{Fe}_3\text{O}_4$ -PEI-naringinase and free naringinase.

**3.3.3 Storage stability of immobilized naringinase.** The storage stability of the immobilized naringinase and free naringinase was shown in Fig. 10, indicating that the immobilized naringinase retained more than 80% of the relative naringinase activity after 30 days of storage, which may be due to the multi-point covalent binding of naringinase on these particles, so that naringinase maintained a stable configuration.<sup>37</sup> On the contrary, the enzyme activity of free naringinase was significantly reduced during storage (relative enzyme activity left was less than 30% in 30 days of storage). The results illuminated that  $\text{Fe}_3\text{O}_4$ -PEI immobilized naringinase had excellent application potential, especially when the enzyme needed to be transported and stored for long distances.<sup>43</sup>

## 4. Conclusion

In this study, we prepared polyethyleneimine (PEI) modified  $\text{Fe}_3\text{O}_4$  magnetic nanoparticles using co-precipitation method, and the magnetic nanoparticles were used for naringinase immobilization. The immobilized naringinase activity reached 690.74 U per g-support, as the pH of 5.5, temperature of 35 °C, immobilization time of 4 h, and the initial naringinase activity of 406.25 U mL<sup>-1</sup>. Through the study of the enzymatic properties of the immobilized enzyme, it was found that the enzyme activity of the immobilized enzyme could reach the highest value of 710.97 U per g-support under the optimized reaction temperature of 60 °C and pH of 5.5. The naringinase activity was much higher than those of the previous works. Meanwhile, the naringinase-carrying rate and naringinase activity recovery of  $\text{Fe}_3\text{O}_4$ -PEI immobilized naringinase were 92.93% and 20.89%, respectively. Compared with free naringinase, the pH stability and thermal stability of  $\text{Fe}_3\text{O}_4$ -PEI immobilized naringinase was greatly improved. In addition,  $\text{Fe}_3\text{O}_4$ -PEI-naringinase still kept 60.58% relative enzyme activity after ten cycles use. Furthermore, the immobilized naringinase maintained 87.52% of relative enzyme activity after one month of storage at 4 °C. It was shown that the  $\text{Fe}_3\text{O}_4$ -PEI immobilized naringinase had good operational stability and storage stability. As a novel enzyme

immobilization material,  $\text{Fe}_3\text{O}_4$ -PEI magnetic nanoparticles had achieved significant progress in the improvement of enzyme activity reusability and storage stability, and made it possible to the application of magnetic nanomaterial technology in the field of immobilized enzymes.

## Author contributions

Chan Yu: data curation, writing – original draft. Jing Tian: writing – review & editing. Honglei Zhan: writing – review & editing. Xinyu Zheng: data curation. Shujing Wang: data curation. Qian Li & Xitong Sun & Xiyun Sun: conceptualization, funding acquisition, writing – review & editing.

## Conflicts of interest

The authors declare that they have no known competing financial interests or personal relationships that could have appeared to influence the work reported in this paper.

## Acknowledgements

This work was supported by the National Natural Science Foundation of China (No. 31601411, No. 21804129 and No. 31771914), Scientific Research Project of Liaoning Provincial Department of Education (No. J2020043 & No. J2020096) and Key Projects of Liaoning Natural Science Foundation Program (No. 20180540130). We are grateful for the test analysis support from Analysis Center of Dalian Polytechnic University.

## References

- 1 M. H. Ribeiro, Naringinases: occurrence, characteristics, and applications, *Appl. Biochem. Biotechnol.*, 2011, **90**, 1883–1895.
- 2 L. Caraveo, H. Medina, I. Rodríguez-Buenfil, *et al.*, A simple plate-assay for screening extracellular naringinase produced by streptomycetes, *J. Microbiol. Methods*, 2014, **102**, 8–11.
- 3 M. Puri, Updates on naringinase: structural and biotechnological aspects, *Appl. Biochem. Biotechnol.*, 2012, **93**, 49–60.
- 4 M. E. Khosroshahi and L. Ghazanfari, Synthesis of three-layered magnetic based nanostructure for clinical application, *Int. J. Nanosci. Nanotechnol.*, 2011, **7**, 57–64.
- 5 G. E. A. Awad, E. A. A. A. Abd, A. N. Shehata, *et al.*, Covalent immobilization of microbial naringinase using novel thermally stable biopolymer for hydrolysis of naringin, *Biotech*, 2016, **6**, 14.
- 6 M. D. Busto, V. Meza, N. Ortega, *et al.*, Immobilization of naringinase from *Aspergillus niger* CECT 2088 in poly(vinyl alcohol) cryogels for the debittering of juices, *Food Chem.*, 2007, **104**, 1177–1182.
- 7 S. Lei, Y. Xu, G. Fan, *et al.*, Immobilization of naringinase on mesoporous molecular sieve MCM-41 and its application to debittering of white grapefruit, *Appl. Surf. Sci.*, 2011, **257**, 4096–4099.





- 8 F. Soria, G. Ellenrieder and G. B. Oliveira,  $\alpha$ -l-Rhamnosidase of *Aspergillus terreus* immobilized on ferromagnetic supports, *Appl. Microbiol. Biotechnol.*, 2012, **93**, 1127–1134.
- 9 M. I. Amaro, J. Rocha, H. Vila-Real, *et al.*, Anti-inflammatory activity of naringin and the biosynthesised naringenin by naringinase immobilized in microstructured materials in a model of DSS-induced colitis in mice, *Food Res. Int.*, 2009, **42**, 1010–1017.
- 10 Q. Liu, L. Lu and M. Xiao, Cell surface engineering of  $\alpha$ -l-rhamnosidase for naringin hydrolysis, *Bioresour. Technol.*, 2012, **123**, 144–149.
- 11 M. A. P. Nunes, H. Vila-Real, P. C. B. Fernandes, *et al.*, Immobilization of naringinase in PVA-alginate matrix using an innovative technique, *Appl. Biochem. Biotechnol.*, 2010, **160**, 2129–2147.
- 12 M. Misson, H. Zhang and B. Jin, Nanobiocatalyst advancements and bioprocessing applications, *J. R. Soc., Interface*, 2015, **12**, 20140891.
- 13 M. M. Nikje, L. Sarchami and L. Rahmani, Fabrication of 2-chloropyridine functionalized  $\text{Fe}_3\text{O}_4$ /amino-silane core-shell nanoparticles, *Int. J. Nanosci. Nanotechnol.*, 2015, **11**, 39–44.
- 14 M. E. Khosroshahi and L. Ghazanfari, Preparation and characterization of silica-coated iron-oxide bionanoparticles under  $\text{N}_2$  gas, *Phys. E*, 2010, **42**, 1824–1829.
- 15 C. G. C. M. Netto, H. E. Toma and L. H. Andrade, Superparamagnetic nanoparticles as versatile carriers and supporting materials for enzymes, *J. Mol. Catal. B: Enzym.*, 2013, **85–86**, 71–92.
- 16 M. L. Verma, M. Naebe, C. J. Barrow, *et al.*, Enzyme immobilisation on amino-functionalised multi-walled carbon nanotubes: structural and biocatalytic characterisation, *PLoS One*, 2013, **8**, e73642.
- 17 A. Xiao, H. You, C. Wu, *et al.*, Immobilization and characterization of naringinase from *Aspergillus aculeatus* onto magnetic  $\text{Fe}_3\text{O}_4$  nanoparticles, *Nanosci. Nanotechnol. Lett.*, 2015, **7**, 770–778.
- 18 T. Homa and M. Mohaddeseh, Nano-magnetic cross-linked enzyme aggregates of naringinase an efficient nanobiocatalyst for naringin hydrolysis, *Int. J. Biol. Macromol.*, 2018, **117**, 134–143.
- 19 T. Homa and M. Mohaddeseh, Kinetic and thermodynamic features of nanomagnetic cross-linked enzyme aggregates of naringinase nanobiocatalyst in naringin hydrolysis, *Int. J. Biol. Macromol.*, 2018, **119**, 717–725.
- 20 C. Ming, G. Zeng, P. Xu, *et al.*, How do enzymes 'meet' nanoparticles and nanomaterials, *Trends Biochem. Sci.*, 2017, **42**, 914–930.
- 21 M. Khoobi, S. F. Motevalizadeh, Z. Asadgol, *et al.*, Synthesis of functionalized polyethylenimine-grafted mesoporous silica spheres and the effect of side arms on lipase immobilization and application, *Biochem. Eng. J.*, 2014, **8**, 131–141.
- 22 M. Khoobi, S. F. Motevalizadeh, Z. Asadgol, *et al.*, Polyethyleneimine-modified superparamagnetic  $\text{Fe}_3\text{O}_4$  nanoparticles for lipase immobilization: Characterization and application, *Mater. Chem. Phys.*, 2015, **149–150**, 77–86.
- 23 J. J. Virgen-Ortíz, J. D. Santos, Á. Berenguer-Murcia, *et al.*, Polyethylenimine: A very useful ionic polymer in the design of immobilized enzyme biocatalysts, *J. Mater. Chem. B*, 2017, **5**, 7461–7490.
- 24 C. Cui, Y. Tao, L. Li, *et al.*, Improving the activity and stability of *Yarrowia lipolytica* lipase Lip2 by immobilization on polyethyleneimine-coated polyurethane foam, *J. Mol. Catal. B: Enzym.*, 2013, **91**, 59–66.
- 25 L. Yang, C. Guo, L. Jia, *et al.*, Fabrication of biocompatible temperature- and pH-responsive magnetic nanoparticles and their reversible agglomeration in aqueous milieu, *Ind. Eng. Chem. Res.*, 2010, **49**, 8518–8525.
- 26 H. Vila-Real, A. J. Alfaia, M. E. Rosa, *et al.*, An innovative sol-gel naringinase bioencapsulation process for glycosides hydrolysis, *Process Biochem.*, 2010, **45**, 841–850.
- 27 H. A. L. Pedro, A. J. Alfaia, J. Marques, *et al.*, Design of an immobilized enzyme system for naringin hydrolysis at high-pressure, *Enzyme Microb. Technol.*, 2007, **40**, 442–446.
- 28 M. Busto, V. Meza, N. Ortega, *et al.*, Immobilization of naringinase from *Aspergillus niger* CECT 2088 in poly(vinyl alcohol) cryogels for the debittering of juices, *Food Chem.*, 2007, **104**, 1177–1182.
- 29 P. W. Cui, J. Li, Z. Xiao, *et al.*, Immobilization of penicillium sp. naringinase on epoxy resin, *Food Ferment. Ind.*, 2014, **40**, 87–92.
- 30 J. C. Zhang, L. W. Wang, S. Y. Liu, *et al.*, Synthesis, characterization, and cytotoxicity of mixed-ligand complexes of palladium(II) with 1,10-phenanthroline and *N*-carbonyl-L-isoleucine dianion, *Russ. J. Coord. Chem.*, 2014, **40**, 115–119.
- 31 M. Kalantari, M. Kazemeini, F. Tabandeh, *et al.*, Lipase immobilisation on magnetic silica nanocomposite particles: effects of the silica structure on properties of the immobilised enzyme, *J. Mater. Chem.*, 2012, **22**, 8385–8393.
- 32 P. Esmailnejad-Ahranjani, M. Kazemeini, G. Singh, *et al.*, Amine-functionalized magnetic nanocomposite particles for efficient immobilization of lipase: effects of functional molecule size on properties of the immobilized lipase, *RSC Adv.*, 2015, **5**, 33313–33327.
- 33 X. Sun, L. Yang, Q. Li, *et al.*, Amino-functionalized magnetic cellulose nanocomposite as adsorbent for removal of Cr(VI): synthesis and adsorption studies, *Chem. Eng. J.*, 2014, **241**, 175–183.
- 34 M. A. Diab, A. Z. El-Sonbati and D. M. Bader, Thermal stability and degradation of chitosan modified by acetophenone, *J. Polym. Environ.*, 2012, **20**, 29–36.
- 35 B. Hu, J. Pan, H. L. Yu, *et al.*, Immobilization of *Serratia marcescens* lipase onto amino-functionalized magnetic nanoparticles for repeated use in enzymatic synthesis of diltiazem intermediate, *Process Biochem.*, 2009, **44**, 1019–1024.
- 36 L. Fernando, M. G. Jose and L. Betancor, Glutaraldehyde-mediated protein immobilization, *Methods Mol. Biol.*, 2013, **1051**, 33–41.
- 37 J. Pan, X. D. Kong, C. X. Li, *et al.*, Crosslinking of enzyme coaggregate with polyethyleneimine: A simple and promising method for preparing stable biocatalyst of



- Serratia marcescens* lipase, *J. Mol. Catal. B: Enzym.*, 2011, **68**, 256–261.
- 38 L. Fernando, L. Betancor, A. Hidalgo, *et al.*, Co-aggregation of enzymes and polyethyleneimine: a simple method to prepare stable and immobilized derivatives of glutaryl acylase, *Biomacromolecules*, 2005, **6**, 1839.
  - 39 W. Huang, Y. Zhan, X. Shi, *et al.*, Controllable immobilization of naringinase on electrospun cellulose acetate nanofibers and their application to juice debittering, *Int. J. Biol. Macromol.*, 2017, **98**, 630–636.
  - 40 J. Luo, Q. Li, X. Sun, *et al.*, The study of the characteristics and hydrolysis properties of naringinase immobilized by porous silica material, *RSC Adv.*, 2019, **9**, 4514–4520.
  - 41 J. Jordan, C. S. S. R. Kumar and C. Theegala, Preparation and characterization of cellulase-bound magnetite nanoparticles, *J. Mol. Catal. B: Enzym.*, 2011, **68**, 139–146.
  - 42 D. Li, W. Y. Teoh, J. J. Gooding, *et al.*, Functionalization strategies for protease immobilization on magnetic nanoparticles, *Adv. Funct. Mater.*, 2010, **20**, 1767–1777.
  - 43 F. Zhang, R. Wang, C. Zhen, *et al.*, Magnetic cellulose nanocrystals: synthesis by electrostatic self-assembly approach and efficient use for immobilization of papain, *J. Mol. Catal. B: Enzym.*, 2016, **134**, 164–171.

